Structural Changes of Lignin in Soda Delignification Process and Associations with Pollution Load

Yuhui Xue, Youming Li, Zhuang Liu, and Yi Hou *

Dissolved lignin in eucalyptus black liquor was obtained at five different reaction times (1 h to 5 h) throughout the main delignification process to reveal the structural changes of lignin and its contributions to pollution load at different degrees of delignification. During the delignification process, the lignin removal efficiency and Kappa number of the pulp had a clear linear relationship with the holding time at the highest temperature (170 °C). This indicated that the degree of delignification to which the pulp could be regulated by the holding time. Condensation and degradation appeared to participate as two competitive reactions in the cooking process. The condensation structures of lignin increased remarkably in the first 3 h, which resulted in increased molecular weight. Then, the degradation of lignin became the main reaction at longer reaction times (4 h to 5 h), when the β-O-4' and β–β' bonds were dramatically broken. Furthermore, the lignin concentration in black liquor increased with delignification time, which had a positive correlation to chemical oxygen demand (CODcr) in black liquor. The proportion of CODcr produced by lignin increased remarkably in the decomposition stage of lignin, which revealed the importance of changes in the lignin structure during the delignification process to the pollution load.

Keywords: HSQC-NMR; Lignin; Pollution load; Structural changes

*Contact information: State Key Laboratory of Pulp and Paper Engineering, South China University of Technology, Guangzhou 510640, P.R. China; *Corresponding author: ceyhou@scut.edu.cn*

INTRODUCTION

Due to high pollution loads and chromatic contributors, the pulp and paper industry is facing heavy pressure to decrease its pollution. Pulp and paper mill wastewater with high color, biochemical oxygen demand (BOD5), and chemical oxygen demand (CODcr) easily leads to serious contamination of clean water and soil (Haq *et al.* 2016; Xin *et al.* 2018). Alkaline delignification is an efficient treatment for removing lignin from un-treated biomass in the factory. During alkaline treatment, lignin will dissolve into black liquor, which is a major contaminant of wastewater (Minu *et al.* 2012).

Recently, researchers have reported structural changes of lignin in alkaline solution treatment. Das *et al.* (2019) reported that a low molecular weight fraction of lignin was removed after alkaline pretreatment. However, lignin showed a condensation process with the pretreatment of steam explosion, leading to an increase in condensed lignin structures. The study by Baptista *et al.* (2008) showed that the residual lignin structure was influenced by the method of pulping process and the degree of delignification. Although it can be concluded that the functional groups of lignin, the condensation degree, and the molecular mass were influenced by the degree of delignification, the relationship between the degradation degree and the contribution of the product on the pollution load needs to be demonstrated in depth.

Eucalyptus was chosen as the raw material. The soda-method was applied for delignification, and five time points during the course of batch cooking experiments (1 h to 5 h) were selected to cover the main degree of delignification. Meantime, the lignin structure changes at different delignification time and the influence of delignification degree on pollution load were determined.

EXPERIMENTAL

Materials

Eucalyptus (lignin content 21.7%, cellulose 44.4%, and hemicellulose 36.9%) was harvested from a commercial forest farm on Paiyang Mountain (Guangxi, China). The wood chips were cut into slices approximately 3 cm to 5 cm in width and 2 mm to 4 mm thickness after removing the barks.

Soda pulping

The conditions of soda cooking or delignification were as follows: the maximum temperature was 170 °C, the ratio of liquor-to-wood was 5:1 (v/wt), and the active alkali charge was 30%. Wood slices were heated using a computer-controlled vertical reactor (Greenwood Corporation, Greenville, SC, USA) for 75 min from room temperature to 170 °C and kept for 1 h, 2 h, 3 h, 4 h, and 5 h. The pulps were washed and stored in the refrigerator to test the Kappa number.

Lignin separation from black liquor

Lignin was precipitated from black liquor by adjusting the pH to 2 with 2 mol/L H_2SO_4, and stirred for 1 h at 55 °C. Then, the mixture was centrifuged to separate lignin at 4000 rpm for 15 min. The solid residue of lignin was collected and washed with deionized water until the wash water was neutral, then dried in the vacuum oven for 48 h, during which the temperature was not allowed to exceed 40 °C. All experiments were performed in triplicate.

Methods

Elemental analysis

The elemental compositions of lignin were established by an Elementar Vario EL cube instrument (Elementar Corp., Berlin, Germany), which gave the percentage contents of carbon, hydrogen, nitrogen, and sulfur after high-temperature combustion of the samples. The oxygen content was calculated from the difference between the sample weight and the C, H, and N contents.

Gel permeation chromatography

Gel permeation chromatography (Waters 515; Waters Corporation, Milford, MA, USA) with a Waters Styragel HT3 column was tested to obtain the molecular weight distributions of lignin (Liu *et al.* 2018). The lignin samples were dissolved in tetrahydrofurane (THF) (1 mg/mL) and filtered (pore size: 0.22 mm) to avoid plugging of the columns from large impurities. The column temperature was maintained at 40 °C with a flow rate of 1 mL THF/min. The calibration curve was made by running polystyrene standards with a molecular weight range from 2,000 Da to 100,000 Da.

2-Dimensional (2D) heteronuclear single quantum correlation (HSQC) Nuclear Magnetic Resonance (NMR)

The 2D HSQC NMR spectra were recorded in HSQC experiments (Bruker Co., Ettlingen, Germany). A 100 mg amount of lignin was dissolved in 0.5 mL of dimethyl sulfoxide (DMSO-d6). The spectral widths were 5000 Hz and 20000 Hz for the ^{1}H and ^{13}C dimensions, respectively. The number of collected complex points was 1024 for the ^{1}H dimension with a recycle delay of 1.5 s. The number of transients was 64, and 256 time increments were recorded in the ^{13}C dimension in the experiment. The 1JCH used was 145 Hz. Prior to Fourier transformation, the data matrices were zero-filled to 1024 points in the ^{13}C dimension. Data processing was performed using standard Bruker Topspin-NMR software (Bruker Co., Ettlingen, Germany).

Kappa number

The Kappa number of the pulps was determined according to the TAPPI T236 cm-85 (2002) standard.

Lignin removal efficiency

The lignin removal efficiency during the soda delignification process was calculated according to the following equation:

$$\text{Lignin removal efficiency} = \frac{\text{Lignin in raw material-Lignin in pulp}}{\text{Lignin in raw material}} \quad (1)$$

CODcr

The CODcr evaluation of black liquor was performed using a spectrophotometer (DR2800; Hach, Loveland, CO, USA) according to the protocols of Hach Lange kits (Walter 1961).

Determination of lignin concentration in black liquor

To determine the lignin concentration in black liquor, an ultraviolet spectrophotometer (DR6000; Hach, Loveland, CO, USA) absorbance analytic method (Hou *et al*. 2018) was used to establish the relationship between lignin concentration and UV absorbance.

Determination of the contribution of lignin in black liquor to CODcr

The testing method was based on previous research (Wei *et al.* 2018). Lignin was dissolved in a 3,5-dinitrosalicylic acid (DNS) solution to prepare solutions of different concentrations of solution and its absorbance was measured using a DR2800 Hach spectrophotometer to obtain a standard curve of lignin concentration and absorbance.

RESULTS AND DISCUSSION

To express and facilitate the comprehension of the following figures and tables, 1 h, 2 h, 3 h, 4 h, and 5h – soda lignin or pulp was obtained with different delignification times; '1 h' represented a holding time of 1 h at maximum temperature.

Relationship between Delignification Time and Lignin Removal Efficiency

Lignin removal efficiency was calculated. Changes in the trends of lignin removal efficiency and the Kappa number of pulps during the delignification process are shown, respectively, in Fig. 1.

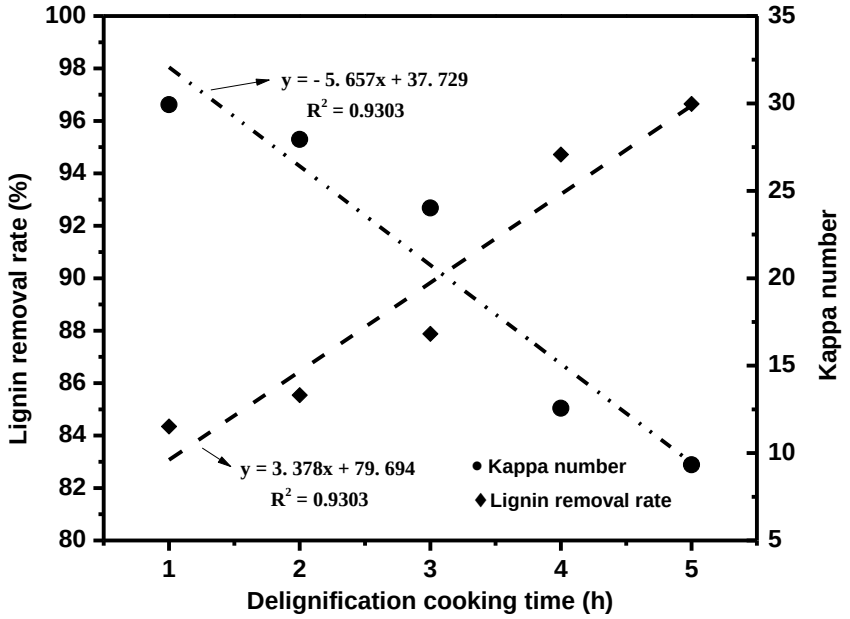

Fig. 1. Relationship of the delignification time, removal efficiency of lignin, and Kappa number of pulps during the delignification process

The lignin removal efficiencies at different delignification times were 84.4%, 85.5%, 87.9%, 94.7%, and 96.6%. With prolonged delignification time, lignin removal efficiencies gradually increased, and the removal rate of lignin had a positive linear relationship to delignification time. It should be noted that the rate of lignin removal for 1 h to 3 h was among 84% to 87%, which was smaller than 4 h (94.7%) and 5 h (96.6%), which showed that its compact and stable structure made it difficult to be removed.

Figure 1 shows that the Kappa numbers of pulps exhibited a negative correlation with the delignification time. The decreased Kappa number was attributable to the dissolving of lignin from wood into black liquor.

A large amount of dissolution lignin occurred from 3 h (lignin removal efficiency 87.88%) to 4 h (lignin removal efficiency 94.72%) resulting in sharp drops in the Kappa number at this stage, which hinted at the changes of dissolution behavior of lignin at this stage. The linear relationships of lignin removal and the Kappa number of pulps to the delignification times suggested that in the cooking process the degree of delignification could be easily regulated by the heating time.

Elemental Analysis

Table 1 shows the elemental analysis of the lignin samples, and obvious differences in the elemental content of lignin obtained from different degrees of cooking can be noticed.

Table 1. Element Analysis and C9 Empirical Formulas of Lignins from Different Delignification Times

Sample	C (%)	H (%)	O[a] (%)	N (%)	C9 Formula[b]	Degree of Unsaturation	C/H	HHV[c]
1 h	53.20	5.79	40.77	0.07	$C_9H_{11.75}O_{5.17}N_{0.01}$	4.13	9.19	19.00
2 h	57.75	5.76	36.34	0.07	$C_9H_{10.77}O_{4.25}N_{0.01}$	4.62	10.03	21.30
3 h	58.38	5.82	35.76	0.05	$C_9H_{10.77}O_{4.13}N_{0.003}$	4.62	10.04	21.70
4 h	62.95	5.72	31.13	0.06	$C_9H_{9.81}O_{3.35}N_{0.01}$	5.10	11.01	23.93
5 h	63.88	5.94	30.12	0.06	$C_9H_{10.04}O_{3.18}N_{0.007}$	4.98	10.76	24.75

[a] Calculated by the difference; [b] Calculated on the basis of elemental composition; [c] HHV = 0.3383 × C + 1.442 × (H − O/8) (KJ/kg) (Zhao *et al*. 2011); HHV- High heat value

The carbon content in the five lignin samples was 53.2%, 57.8%, 58.4%, 63.0%, and 63.9%, which showed an increasing trend, while the content of hydrogen saw a leveling off. It showed that the oxygen content decreased from 40.8% to 30.1%, indicating that breakage of the chemical bonds of hydroxyl, methoxy, and ether linkages occurred during the delignification process (Jiang *et al.* 2018), which resulted in an increase in the HHV value of lignin. The degree of unsaturation of the samples was in the range of 4.13 to 5.10. Generally, the unsaturation of a benzene ring is 4, and the degree of unsaturation increased by 1 for each additional conjugated double bond. It could be inferred that the values of 4.13 to 5.10 proved that many dehydration condensation reactions occurred to form some unsaturated bonds during alkaline treatment, which was consistent with the results of the previous study (Wen *et al*. 2013b; Jiang *et al*. 2018).

Molecular Weight Analysis

In this study, the effects of delignification time on the distribution of degraded fragments from different lignin fractions were investigated as shown in Fig. 2 and Table 2.

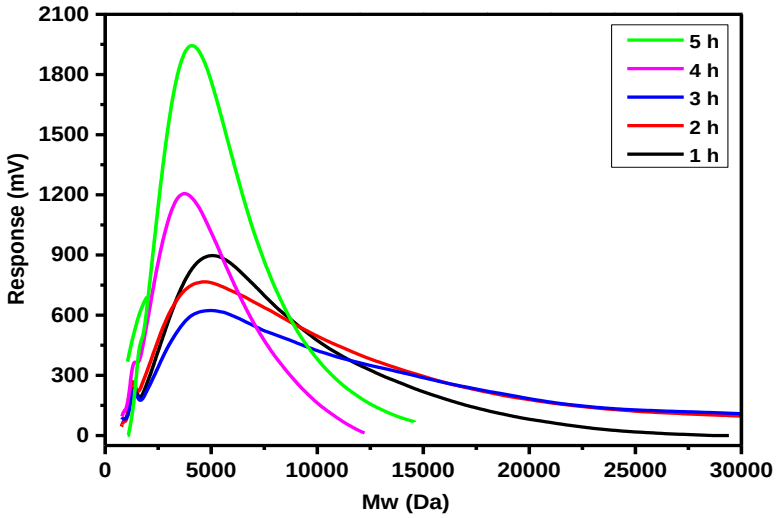

Fig. 2. Molecular weight distribution of different isolated lignin samples

It was clear that the degree of delignification had an effect on the molecular weight distribution of lignin. With the prolonging of soaking time, the molecular weight distribution curve gradually shifted towards the low-Mw region, and the molecular weight distribution of lignin in the first 3 h was relatively wide, from 0 DA to 30000 DA. However, samples with deep delignification, such as those with delignification times of 4 h and 5 h, had a narrow molecular weight distribution, which only ranged from 0 DA to 15000 DA, and approximately 80% of the molecular weight rested in the range of 2000 DA to 8000 DA.

Table 2. Results of Percentages of Different Molecular Weights of Lignin, Weight-average (M_w), Number-average (M_n), Molecular Weights, and Polydispersity Indexes (M_w/M_n) of the Isolated Lignin Samples

Sample	> 15000[a]	15000 to 8000	8000 to 5000	5000 to 2000	< 2000	M_n	M_w	Polymer Dispersity (PD)
1 h	3.76	18.74	27.02	40.32	10.16	3878	5923	1.53
2 h	10.12	18.91	21.95	37.20	11.82	3840	7290	1.90
3 h	12.82	19.84	21.67	34.01	11.66	3973	8351	2.03
4 h	0.00	4.82	20.54	57.90	16.74	3772	7222	1.91
5 h	0.00	8.30	24.96	58.91	7.73	3100	4183	1.35

[a] The values in the second to eighth columns are the percentages of molecular weight in different ranges

The lignin M_w from 1 h to 3 h were 5923, 7290, and 8351, respectively, and the PD value was calculated to be 1.53, 1.90, and 2.03. These findings indicated an increasing trend of M_w and that a broader distribution of lignin molecules was obtained in the first 3 h. It was reported that the condensation reaction of the degraded lignin occurred easily in the alkaline condition to form a new product with a larger M_w at a high temperature (Sun and Xue 2018). As can be seen from Table 2, in the first 3 h, the ratio of the molecular weight range '> 15000' increased, which was consistent with the trend of M_w and DP changes. However, when the cooking time was extended to 4 h and 5 h, no molecular weight of '> 15000' could be observed and the proportion of molecular weight '< 2000' increased to 16.74%. This indicated that a large amount of lignin was degraded to smaller molecules at this stage.

Simultaneously, this study obtained a fitted quadratic polynomial relationship between lignin removal efficiency and molecular weight during the delignification process as shown in Fig. 3. As the delignification rate increased from 84.4% to 96.6%, the molecular weight of lignin increased from 5923 to 8351 and then decreased to 4183. The molecular weight of lignin first increased and then decreased with the extension of delignification time, which also indicated that lignin dissolved in the black liquor may experience the reactions of condensation and degradation simultaneously and competitively during the NaOH treatment. Condensation may be the main reaction in the first 3 h, and then the degradation reaction was more prominent in the last 2 h, which is consistent with the conclusion of GPC and 2D NMR.

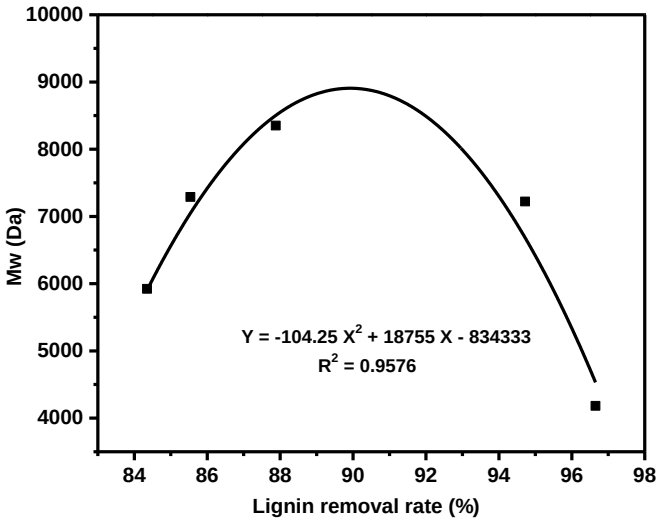

Fig. 3. The relationship between lignin removal efficiency of raw material and the Mw of lignin

2D-HSQC Analysis

The 2D-HSQC NMR can provide useful structural information of lignin, including substructures (inter-coupling bonds) and the S/G ratio. Therefore, to further elucidate the structural changes of lignin that were obtained from different cooking times, the 2D-HSQC spectra of all samples were investigated. The degree of delignification had a remarkable effect on the chemical structure of lignin. The aliphatic region (δC/δH 50 to 90/2.5 to 6.0) and aromatic regions (δC/δH 90 to 135/5.5 to 8.5) in the HSQC spectra are shown in Fig. 4. The main lignin substructures identified from the HSQC analysis are shown in Table 3. Core substructures were assigned according to previous reports (Ibarra *et al.* 2007; Yuan *et al.* 2011; Fernández-Costas *et al.* 2014; Lei *et al.* 2019), which are listed in Table 4.

Table 3. Substructures of Lignin, Including Main Aromatic Units and Condensation Structures Identified by 2D NMR

Structural Formula	Assignment	Structural Formula	Assignment	Structural Formula	Assign-ment
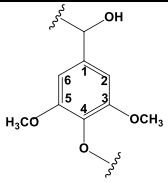 S	(S) Syringyl unit	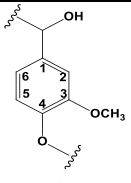 G	(G) Guaiacyl unit	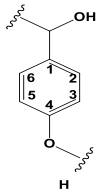 H	(H) p-Hydroxyphenyl unit
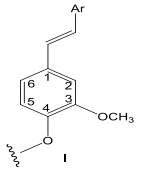 I	(I) stilbene substructures	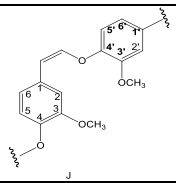 J	(J) Vinyl aryl ethers	K	(K) Diaryl ethers
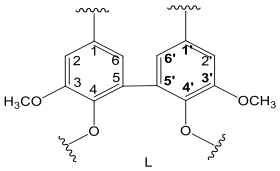 L	(L) Biphenyl substructures	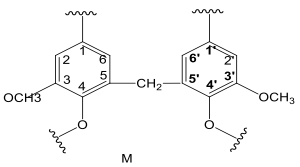 M			(M) Diarylmethylenes

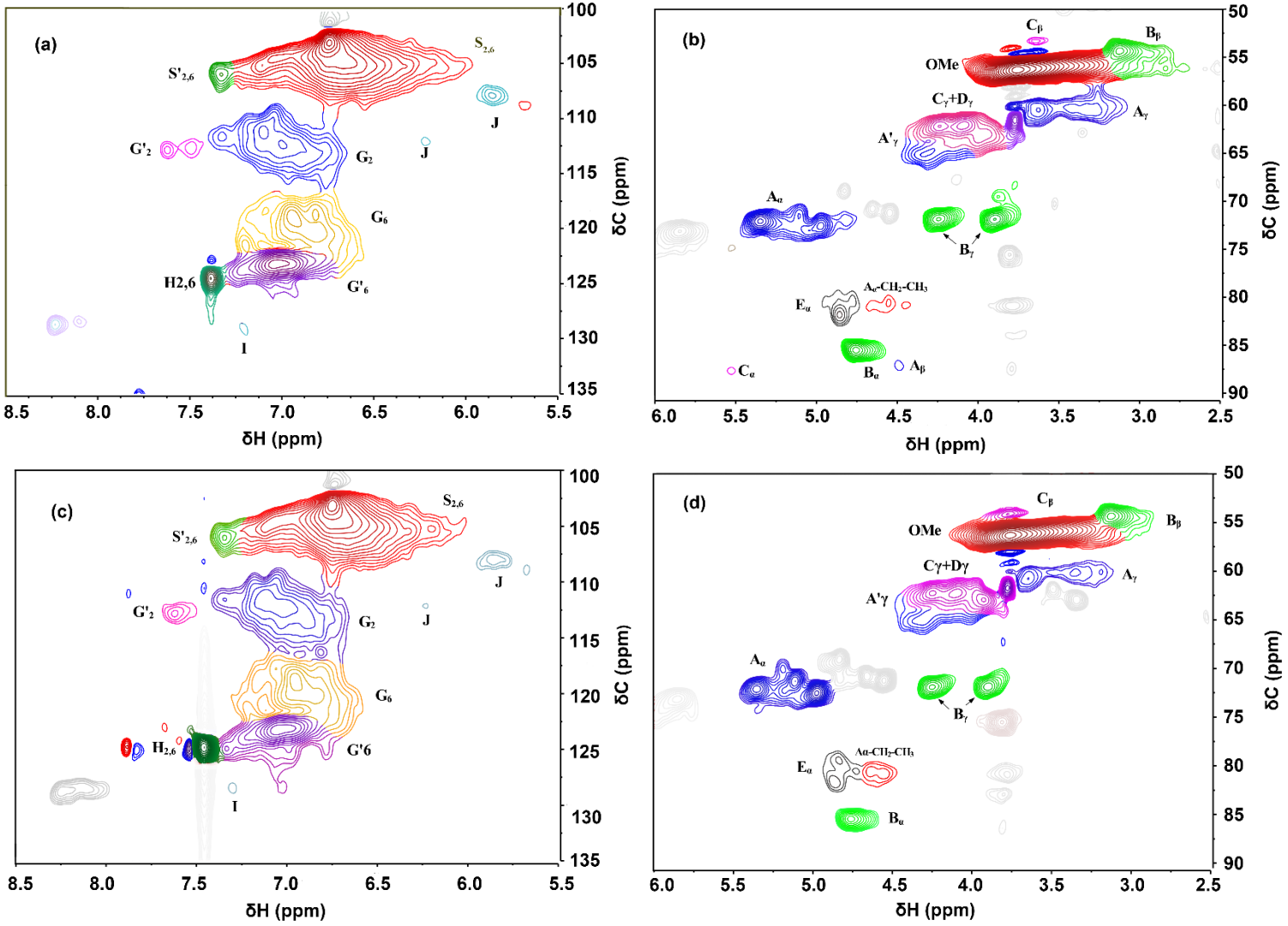
(a)
S'2,6
S2,6
J
G'2
G2
J
G6
H2,6
G'6
I
δH (ppm)
δC (ppm)
(b)
Cβ
Bβ
OMe
Cγ+Dγ
Aγ
A'γ
Aα
Bγ
Aα-CH2-CH3
Eα
Cα
Bα
Aβ
δH (ppm)
δC (ppm)
(c)
S2,6
S'2,6
J
G'2
G2
J
G6
H2,6
G'6
I
δH (ppm)
δC (ppm)
(d)
Cβ
Bβ
OMe
Cγ+Dγ
Aγ
A'γ
Aα
Bγ
Aα-CH2-CH3
Eα
Bα
δH (ppm)
δC (ppm)

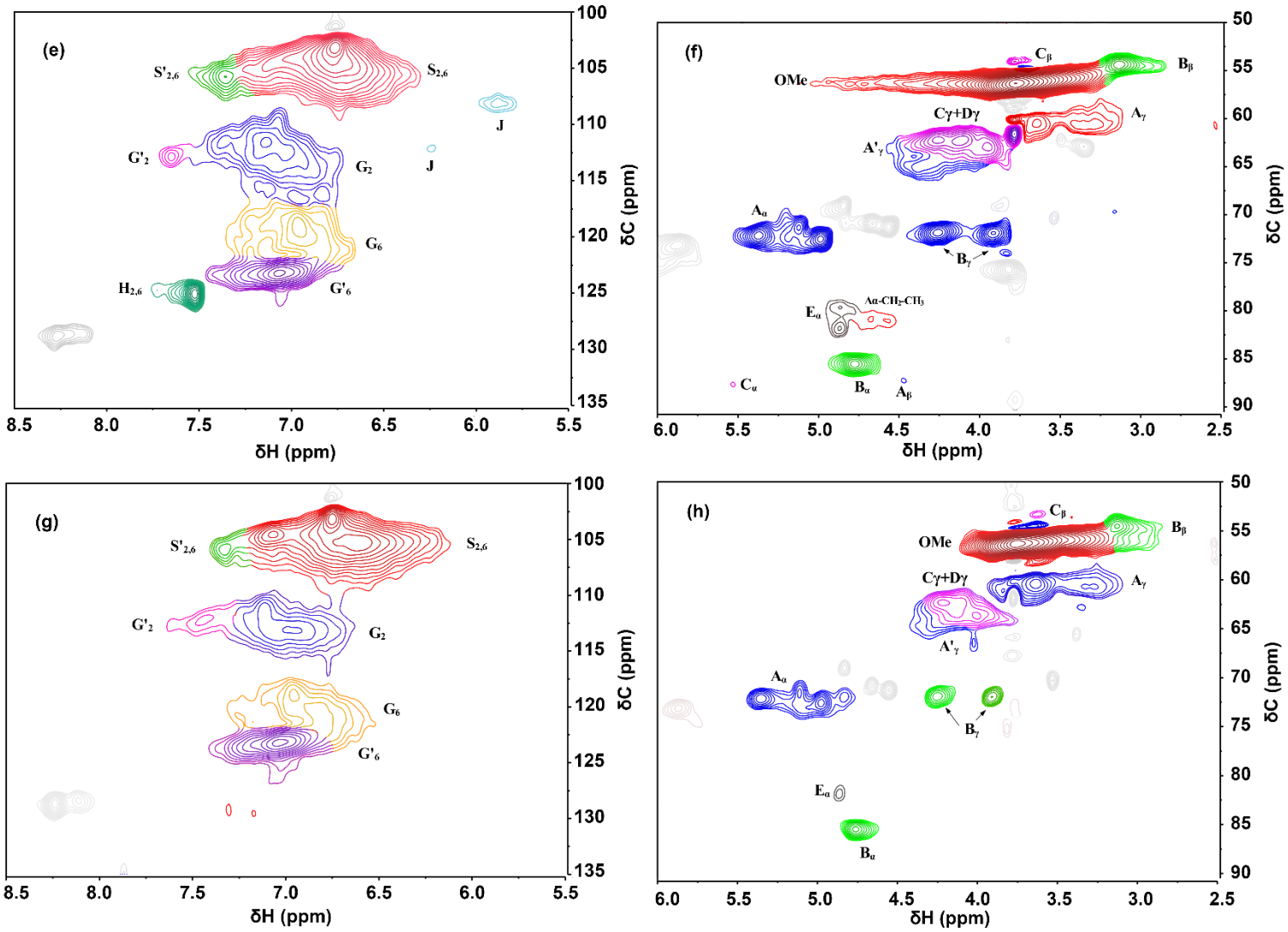
(e)
S'2,6
S2,6
J
G'2
G2
J
G6
H2,6
G'6
δH (ppm)
δC (ppm)
(f)
Cβ
Bβ
OMe
Cγ+Dγ
Aγ
A'γ
Aα
Bγ
Aα-CH2-CH3
Eα
Cα
Bα
Aβ
δH (ppm)
δC (ppm)
(g)
S'2,6
S2,6
G'2
G2
G6
G'6
δH (ppm)
δC (ppm)
(h)
Cβ
Bβ
OMe
Cγ+Dγ
Aγ
A'γ
Aα
Bγ
Eα
Bα
δH (ppm)
δC (ppm)

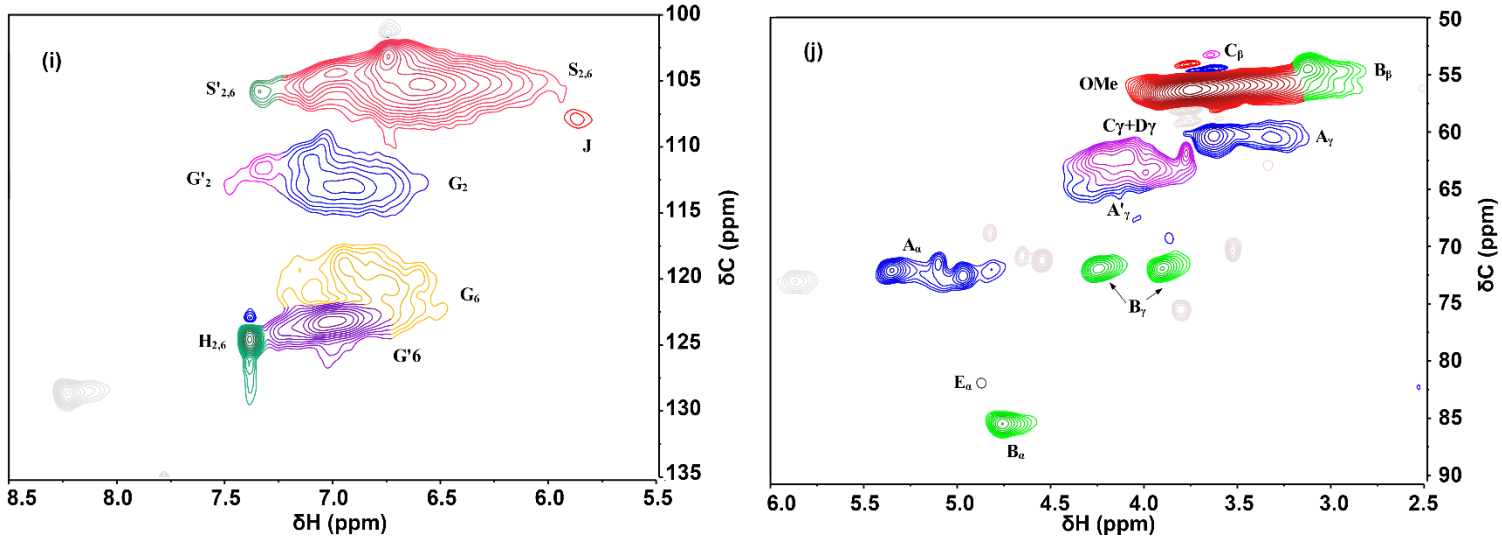

Fig. 4. HSQC spectra of the isolated lignin samples. a(1h), c(2h), e(3h), g(4h), i(5h): aromatic regions (δC/δH 100 to 135/5.5 to 8.5); b(1h), d(2h), f(3h), h(4h), j(5h): aliphatic regions (δC/δH 50 to 90/2.5 to 6.0)

Aliphatic region

The main signals in the aliphatic region of lignin were from -OCH_3, β-O-4′, β-β′, and β-5′. The side-chain regions provided important information about the inter-unit linkages and terminal structures in the lignin together with carbohydrate contamination. The signal for Cβ-Hβ within β-O-4´ in the S unit was seen in δC/δH 87.3/4.4 ppm and the signal at δC/δH 80.5/4.5 ppm due to the presence of α-ethoxylated for β-O-4′ linkage (Aα-CH2-CH3) mainly appeared in the samples of 1 h, 2 h, and 3 h, which was mainly attributed to the depolymerization and cleavage of the lignin in the process of soda cooking when the reaction time exceeded 3 h. Similarly, the disappearance of the phenylcoumaran substructures (C) signal corresponding to Cα-Hα in the spectra of lignin samples in the last 2 h proved that the excessive delignification treatment can lead to cleavage of this linkage.

Aromatic regions

The aromatic regions (δC/δH 90 to 135/5.5 to 8.5) showed remarkable information about the oxidation of side chains of S, G, and H units as well as the S/G ratio of the samples. Figure 4 shows that the signal intensity of S unit was much stronger than that of the G and H units, which implied that lignin obtained *via* acid precipitation from eucalyptus black liquor contained a higher content of S unit, which was well in accordance with the structure of hardwood.

Furthermore, several typical condensed substructures, including stilbene (I), vinyl aryl ethers (J), diaryl ethers (K), biphenyl substructures (L), and diarylmethylenes (M) (δC/δH 20.7/2.1 ppm, not shown) produced during soda pulping were discovered in soda lignin, which was inconsistent with previous publications (An *et al.* 2015). In alkaline pulping, the Cβ-Cγ bond was broken, which indicated that the primary alcohol hydroxyl group at the Cγ position was oxidized to formaldehyde, and the removed formaldehyde acted as a cross-linking agent for the reaction (Pei 2012). Lignin fragments were polymerized together under the action of a crosslinking agent to form a diarylmethylene structure (unit M). The possible condensation reaction path is shown in Fig. 5.

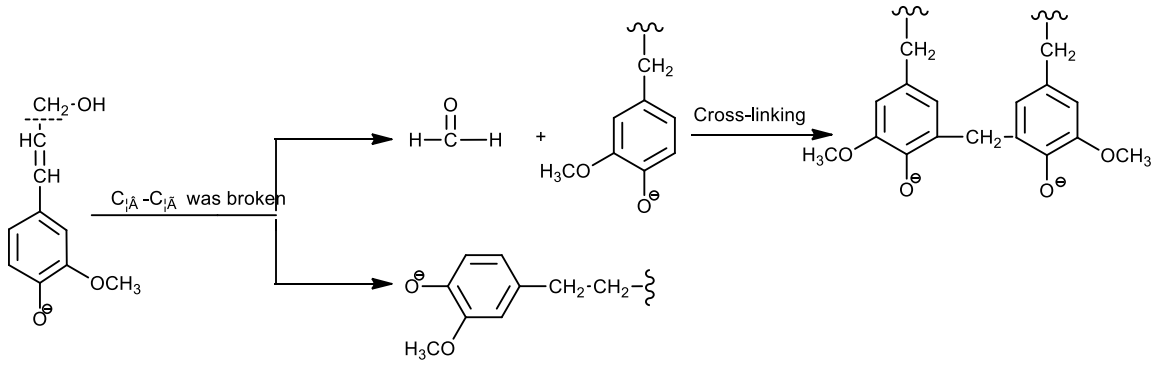

Fig. 5. Path of cross-linking reaction between lignin fragments and formaldehyde

Semiquantitative HSQC analysis

Based on previous calculations (Zhang and Gellerstedt 2011), the major substructures and their abundances in the lignin component were quantitatively estimated. The relative ratios of the β-O-4', β–β', β-5', and S/G ratio linkages could be determined using the aromatic region (100) as an internal standard.

Table 4. Assignments of Signals Observed in $^{1}H/^{13}C$ 2D HSQC NMR Spectra of Lignin Derived from Black Liquor

Labels	δC/δH (ppm)	Assignment
MeO	55.3/3.7	C-H, Methoxyls (MeO)
Aα	72.5/4.9	Cα-Hα, β-O-4′ S Unit (A)
Aβ(S)	87.3/4.4	Cβ-Hβ, β-O-4′ S Unit (A)
Aγ	(59.9/3.3)/(59.9/3.6)	Cγ-Hγ, β-O-4′ Substructures (A)
A'γ	63.7/4.3	Cγ-Hγ, of γ acylated β-O-4′ Substructures (A′)
Bα	85.4/4.7	Cα-Hα, Resinol Substructures (B)
Bβ	54.3/3.1	Cβ-Hβ, Resinol Substructures (B)
Bγ	(71.8/3.8)/(71.8/4.2)	Cγ-Hγ, Resinol Substructures (B)
Cα	87.6/5.5	Cα-Hα, Phenylcoumaran Substructures (C)
Cβ	53.4/3.6	Cβ-Hβ, Phenylcoumaran Substructures (C)
Cγ	62.6/4.0	Cγ-Hγ in Phenylcoumaran Unit (C)
Dγ	62.1/4.2	Cγ-Hγ, Cinnamyl Alcohol End Groups (D)
Eα	81.7/4.8	Cα-Hα, Spirodienone Substructures (E)
Aα-CH2-CH3	80.5/4.5	α-Ethoxylated in β-O-4′ Substructures (Aα-CH2-CH3)
S2,6	103.5/6.7	C2,6-H2,6, (Cα = O) S Units (S′)
S'2,6	106.2/7.3	C2,6-H2,6, Oxidized (Cα = O) S Units (S′)
G2	111.6/7.0	C2-H2, G Units (G)
G'2	112.7/7.5	C2-H2, Oxidized (Cα = O) G Units (G′)
G6	119.2/6.9	C6-H6, G Units (G)
G'6	123.1/7.0	C6-H6, Oxidized (Cα = O) S Units (G′)
H2,6	128.6/7.2	C2,6-H2,6, p-hydroxyphenyl (H)
PB3,5	114.2/6.6	C3,5-H3,5, p-hydroxybenzoate (PB)
Iα/Iβ	128.9/7.2	Cα-Hα and Cβ-Hβ in Stilbene Substructures (I)
Jα	(107.9/5.6)/(112.1/6.2)	Cα-Hα in Vinyl Aryl Ethers (J)
K2	106.9 to 111.29/6.61 to 7.32	C2-H2 in Aryl-O-aryl (4-O-5') Substructures (K)
L6	120.3 to 124.0/6.42 to 7.12	C6-H6 in Biphenyl Substructures (L)
M	20.7/2.1	Diarylmethylene Structure

Table 5. Semiquantitative Results of the Interunit Linkages in Lignins by 2D HSQC Spectra

Sample	β-O-4' (%)	β–β' (%)	β-5' (%)	S/G Ratio
1 h	23.31	10.41	1.04	1.81
2 h	26.36	11.36	0.96	1.63
3 h	28.05	11.98	1.36	1.65
4 h	22.36	6.72	0.54	1.61
5 h	16.42	7.11	0.43	1.59

Five lignin samples showed differences in the ratio of interunit linkages, as shown in Table 5. It should be noted that the relative content of β-O-4′ and β–β' linkage groups in the lignin samples of 1 h to 3 h increased greatly, which implied the formation of additional β-O-4′ and β–β' bonds at an early stage of delignification, which also led to the increase in M_w in the first 3 lignin samples. It also indicated that the condensation reaction among the lignin-degraded fragments generated after the cleavage of the β-O-4', β-β', β-γ' and β-5' bond of lignin occurred in the first 3 h.

Meanwhile, it was noted that with the prolonged delignification time of 4 h and 5 h, the relative content of β-O-4' and β–β' linkage was reduced, suggesting that a lengthy NaOH treatment facilitated the depolymerization of lignin macromolecules. This was most likely due to the fact that β-O-4' together with Cβ-Cβ' linkages were broken into phenolic monomers as well as lignin-derived low-M_w dimers and monomers (Liu *et al.* 2019), which was consistent with the conclusion in the GPC analysis that the high molecular weight (> 15000) percentage of lignin decreased and the low molecular (2000 to 5000) weight fraction increased for 4 h and 5 h.

The S/G (syringyl to guaiacyl) ratio of lignin is an important parameter to evaluate the degree of delignification, especially in hardwood and non-wood biomass (Wen *et al.* 2013a). Obviously, the S/G ratio of lignin decreased with the extension of delignification time, which indicated that S-unit lignin was more easily removed than the G-unit lignin due to the fact that there were two methoxy groups in the S-unit while the G-unit only had one. This resulted in more activity and it was more easily oxidized than the G-unit in an alkaline solution. The result of this discovery was similar with the results reported in published studies (Sun and Xue 2018), which found that the S/G ratios decreased with the prolongation of the treatment time to 3 h, indicating an easier removal of S-unit lignin.

Association of Delignification Degree to Pollution Load and Lignin Structure

Determination of lignin concentration in black liquor

It was obvious that there was a strong linear relationship between lignin concentration and UV absorbance. After calculation, lignin concentrations in black liquor at 1 h to 5 h were 0.23 g/L, 0.24 g/L, 0.41 g/L, 0.64 g/L, and 0.51 g/L, as shown in Table 6.

Table 6. Contribution of Lignin Concentration to CODcr in Black Liquor

Sample	Lignin Concentration in Black Liquor (g/L)	CODcr Produced by Unit Mass Lignin (g/L)	CODcr Produced by Lignin (mg/L)	Total CODcr of Black Liquor (mg/L)	Ratio of CODcr by Lignin (%)
1 h	0.23±0.00	1.34±0.00	32291±50	89895±60	35.92±0.05
2 h	0.24±0.00	1.35±0.00	32882±12	96032±34	34.25±0.02
3 h	0.41±0.01	1.46±0.01	59053±29	159270±25	37.08±0.02
4 h	0.64±0.01	1.59±0.01	101417±46	175582±121	57.76±0.05
5 h	0.51±0.01	1.52±0.01	76901±56	165994±61	46.33±0.04

The lignin concentration in the black liquor increased with the delignification time. When the cooking time was 1 h to 3 h, only the lignin from the middle lamella (ML) and primary wall (P) was dissolved. When the delignification time was prolonged, lignin in the secondary wall (S) that contained a large amount of lignin was dissolved, leading to an

increase in lignin content in black liquor. The lignin content slightly decreased in the last period, which may have been due to the excessive delignification time leading to the break of the aromatic ring.

Contribution of lignin to chemical oxygen demand of black liquor

A positive correlation was found between the lignin concentration and CODcr in black liquor. The amount of CODcr produced by different concentrations of lignin was calculated, as well as the ratio of CODcr produced by lignin for the total CODcr of black liquor. These values are listed in Table 6.

As shown in Table 6, the CODcr produced by lignin increased with increases in lignin concentration, suggesting that the pollution load in black liquor had a strong relationship with the lignin.

The CODcr value produced by the unit mass lignin also showed a trend of first increasing and then slightly decreasing. Thus, similar results were also obtained between the ratio of CODcr produced by lignin in black liquor and delignification time, which implied that the contribution of lignin to the black liquor pollution load changed with the extension of cooking time. The contribution of lignin to CODcr in the first 3 h was approximately 35%, which indicated that the condensation structure of aromatic ring and the aromatic ring was relatively stable, and the actual CODcr that could be oxidized was maintained at a stable level. However, the proportion of CODcr produced by lignin was increased when the lignin entered the decomposition stage, and the molecular weight also began to decrease, showing that lignin was the main source of wastewater pollution.

This study reported a value of 46.3% for the fifth hour, which was lower compared to the fourth hour (57.8%). This was attributed to excessive degradation of carbohydrates caused by "overcooking", and the proportion of CODcr degraded by cellulose and hemicellulose was increased. These results strongly suggested that delignification time had an important impact on CODcr produced by lignin.

Relationship between lignin structure and pollution load

Pola *et al.* (2019) reported that for black liquor, CODcr may result from the contribution of the intermediate produced by the lignin. The GPC analysis in Table 2 and CODcr data Table 5 show that CODcr increased when the percentage of low-M_w (< 2000) of lignin increased, which indicated that the part with low-M_w contributed more to pollution.

Furthermore, the effect of lignin with different C/H ratios on pollution load during the cooking process was investigated. The results indicated that different C/H ratios in the lignin impacted the CODcr of various black liquor. Compared with the data of C/H and CODcr, it was found that the pollution value of wastewater increased with the rise of the C/H ratio of lignin. The lignin with the highest C/H ratio produced the highest yield of CODcr for the 4 h sample.

It was reported (Hu *et al.* 2019) that the C/H ratio affected the formation of the aromatic ring structures. The lignin (4 h) with the highest C/H content produced more aromatics with a relatively smaller ring size, while the sample of 1 h with the lowest C/H content produced more of the aromatics with a relatively bigger ring size. When the size of the aromatic ring compound was large, the oxidizing agent could not completely oxidize the reducing fragments to the lignin degradation product, which resulted in a small CODcr value.

CONCLUSIONS

1. The linear relationships of lignin removal efficiency and the Kappa number of pulps to delignification time indicated that in the cooking process the degree of delignification could be easily regulated by the holding time at the highest temperature.
2. Condensation and degradation were two competitive reactions in the process of alkaline delignification, the lignin condensation was the main reaction in the first 3 h and the degradation reaction was more prominent in the last 2 h.
3. The lignin concentration, CODcr produced by unit concentration of lignin, as well as the proportion of lignin contribution on the total CODcr of black liquor all first increased and then decreased with the extension of delignification time.

ACKNOWLEDGMENTS

The authors are grateful for the support of the National Key R&D project of China 278 (Grant No. 2017YFB0307901) and the National Natural Science Foundation of China 279 (Grant No. 21476091).

REFERENCES CITED

An, Y. X., Li, N., Wu, H., Lou, W. Y., and Zong, M. H. (2015). "Changes in the structure and the thermal properties of kraft lignin during its dissolution in cholinium ionic liquids," *ACS Sustain. Chem. Eng.* 3(11), 2951-2958. DOI: 10.1021/acssuschemeng.5b00915

Baptista, C., Robert, D., and Duarte, A. P. (2008). "Relationship between lignin structure and delignification degree in *Pinus pinaster* kraft pulps," *Bioresource Technol.* 99(7), 2349-2356. DOI: 10.1016/j.biortech.2007.05.012

Das, P., Stoffel, R. B., Area, M. C., and Ragauskas, A. J. (2019). "Effects of one-step alkaline and two-step alkaline/dilute acid and alkaline/steam explosion pretreatments on the structure of isolated pine lignin," *Biomass Bioenerg.* 120, 350-358. DOI: 10.1016/j.biombioe.2018.11.029

Fernández-Costas, C., Gouveia, S., Sanromán, M. A., and Moldes, D. (2014). "Structural characterization of kraft lignins from different spent cooking liquors by 1D and 2D nuclear magnetic resonance spectroscopy," *Biomass Bioenerg.* 63, 156-166. DOI: 10.1016/j.biombioe.2014.02.020

Haq, I., Kumar, S., Kumari, V., Singh, S. K., and Raj, A. (2016). "Evaluation of bioremediation potentiality of ligninolytic *Serratia liquefaciens* for detoxification of pulp and paper mill effluent," *J. Hazard. Mater.* 305, 190-199. DOI: 10.1016/j.jhazmat.2015.11.046

Hou, Y., Sun, Q. H., and Li, Y. M., (2018). "Effect of lignin in red pine wood alkaline pulping black liquor on pollution load," *Journal of Hunan University (Natural Sciences)* 45(6), 155-160. DOI: 10.16339/j.cnki.hdxbzkb.2018.06.024

Hu, X., Guo, H., Gholizadeh, M., Sattari, B., and Liu, Q. (2019). "Pyrolysis of different wood species: Impacts of C/H ratio in feedstock on distribution of pyrolysis products," *Biomass Bioenerg.* 120, 28-39. DOI: 10.1016/j.biombioe.2018.10.021

Ibarra, D., Chávez, M. I., Rencoret, J., Río, J. C. D., Gutiérrez, A., Romero, J., Camarero, S., Martínez, M. J., Jiménez-Barbero, J., and Martínez, A. T. (2007). "Lignin modification during *Eucalyptus globulus* kraft pulping followed by totally chlorine-free bleaching: A two-dimensional nuclear magnetic resonance, Fourier transform infrared, and pyrolysis-gas chromatography/mass spectrometry study," *J. Agr. Food Chem.* 55(9), 3477-3490. DOI: 10.1021/jf063728t

Jiang, B., Zhang, Y., Gu, L., Wu, W., Zhao, H., and Jin, Y. (2018). "Structural elucidation and antioxidant activity of lignin isolated from rice straw and alkali-oxygen black liquor," *Int. J. Biol. Macromol.* 116, 513-519. DOI: 10.1016/j.ijbiomac.2018.05.063

Lei, M., Wu, S., Liang, J., and Liu, C. (2019). "Comprehensive understanding the chemical structure evolution and crucial intermediate radical *in situ* observation in enzymatic hydrolysis/mild acidolysis lignin pyrolysis," *J. Anal. Apply. Pyrol.* 138, 249-260. DOI: 10.1016/j.jaap.2019.01.004

Liu, X., Jiang, Z., Feng, S., Zhang, H., Li, J., and Hu, C. (2019). "Catalytic depolymerization of organosolv lignin to phenolic monomers and low molecular weight oligomers," *Fuel* 244, 247-257. DOI: 10.1016/j.fuel.2019.01.117

Liu, X., Wei, W. Q., Wu, S. B., Lei, M., and Liu, Y. (2018). "A promptly approach from monosaccharides of biomass to oligosaccharides *via* sharp-quenching thermo conversion (SQTC)," *Carbohyd. Polym.* 189, 204-209. DOI: 10.1016/j.carbpol.2018.01.107

Minu, K., Jiby, K. K., and Kishore, V. V. N. (2012). "Isolation and purification of lignin and silica from the black liquor generated during the production of bioethanol from rice straw," *Biomass Bioenerg.* 39(1), 210-217. DOI: 10.1016/j.biombioe.2012.01.007

Pei , J. C. (2012). *Lignocellulosic Chemistry*, China Light Industry Press, Beijng, China.

Pola, L., Collado, S., Oulego, P., and Díaz, M. (2019). "Production of carboxylic acids from the non-lignin residue of black liquor by hydrothermal treatments," *Bioresource Technol.* 284, 105-114. DOI: 10.1016/j.biortech.2019.03.066

Sun, Y. C., and Xue, B. L. (2018). "Understanding structural changes in the lignin of *Eucalyptus urophylla* during pretreatment with an ionic liquid-water mixture," *Ind. Crop. Prod*. 123, 600-609. DOI: 10.1016/j.indcrop.2018.07.029

TAPPI T236 cm-85 (2002). "Pulp Kappa number," TAPPI Press, Atlanta, GA, USA.

Walter, W. G. (1961). "Standard method for the examination of water and wastewater," *American Journal of Public Health & The Nations Health* 51(6), 940. DOI: 10.2105/AJPH.51.6.940-a

Wei, Z. M., Li, Y. M., Cai, F. J., and Hou, Y. (2018). "Contribution of lignin from different bioresources to the pollution load," *BioResources* 13(4), 9053-9065. DOI: 10.15376/biores.13.4.9053-9065

Wen, J.-L., Xue, B.-L., Xu, F., Sun, R.-C., and Pinkert, A. (2013a). "Unmasking the structural features and property of lignin from bamboo," *Ind. Crop. Prod*. 42, 332-343. DOI: 10.1016/j.indcrop.2012.05.041

Wen, J.-L., Yuan, T.-Q., Sun, S.-L., Xu, F., and Sun, R.-C. (2013b). "Understanding the chemical transformations of lignin during ionic liquid pretreatment," *Green Chem.* 16(1), 181-190. DOI: 10.1039/C3GC41752B

Yuan, T.-Q., Sun, S.-N., Xu, F., and Sun, R.-C. (2011). "Characterization of lignin structures and lignin-carbohydrate complex (LCC) linkages by quantitative ^{13}C and 2D HSQC NMR spectroscopy," *J. Agr. Food Chem.* 59(19), 10604-10614. DOI: 10.1021/jf2031549

Zhang, L., and Gellerstedt, G. (2011). "Quantitative 2D HSQC NMR determination of

polymer structures by selecting suitable internal standard references," *Magn. Reson. Chem.* 45(1), 37-45. DOI: 10.1002/mrc.1914

Zhao, X., Wu, R., and Liu, D. (2011). "Production of pulp, ethanol and lignin from sugarcane bagasse by alkali-peracetic acid delignification," *Biomass Bioenerg.* 35(7), 2874-2882. DOI: 10.1016/j.biombioe.2011.03.033

Article submitted: May 20, 2019; Peer review completed: July 21, 2019; Revised version received: July 29, 2019; Accepted; July 31, 2019; Published: August 14, 2019.
DOI: 10.15376/biores.14.4.7869-7885